NANO · MICRO small
www.small-journal.com

# Shedding Light on DNA-Based Nanoprobes for Live-Cell MicroRNA Imaging

*Fan Yang, Huiting Lu, Xiangdan Meng, Haifeng Dong,* and Xueji Zhang*

**DNA-based nanoprobes integrated with various imaging signals have been employed for fabricating versatile biosensor platforms for the study of intracellular biological process and biomarker detection. The nanoprobes developments also provide opportunities for endogenous microRNA (miRNA) in situ analysis. In this review, the authors are primarily interested in various DNA-based nanoprobes for miRNA biosensors and declare strategies to reveal how to customize the desired nanoplatforms. Initially, various delivery vehicles for nanoprobe architectures transmembrane transport are delineated, and their biosecurity and ability for resisting the complex cellular environment are evaluated. Then, the novel strategies for designing DNA sequences as target miRNA specific recognition and signal amplification modules for miRNA detection are presented. Afterward, recent advances in imaging technologies to accurately respond and produce significant signal output are summarized. Finally, the challenges and future directions in the field are discussed.**

## 1. Introduction

MicroRNA (miRNA) molecules are highly conserved modulators and mainly responsible for regulating post-transcriptional gene expression in the cells of human and other animals.[1] These 19–23 nucleotides class of small RNA sequences were first manifested by the discovery of lin-4 in Caenorhabditis elegans in 1993.[2] So far, about 48 860 mature miRNAs distributed in 271 organisms are reported.[3] Increasing evidences have revealed that miRNAs are involved in regulation of about 30% of all genes and almost every genetic pathways.[4] Their transcription regulation mechanism to target gene is described in **Figure 1**: Briefly, mature miRNAs are loaded into an Argonaute (Ago) protein to generate the RNA-induced silencing complex (RISC). Then, the RISC bind to the 3′-untranslated region of target mRNAs with 2–7 nucleotides to induce mRNA degradation or suppress the translation.[5] MiRNAs play pivotal roles in cell development, proliferation, differentiation, apoptosis, and other biological processes.[6] Notably, their dysregulations are involved in numerous human diseases, including malignancies, implying their potential pathological value as new therapeutic indicators in clinical practices.[7]

To date, various technologies for miRNA analysis in vitro including microarray, quantitative real-time polymerase chain reaction (qRT-PCR), Northern blotting, and RNA sequencing.[2] All these technologies displaced the ability to analyze miRNAs via extracted RNA samples from cellular lysate, but ignored cellular heterogeneity and spatio-temporal dynamics information. Alternatively, fluorescent in situ hybridization (FISH) technology enables to profile miRNA spatial distribution in fixed tissues or cells, but with limited throughput.[8] Although the barcode-based FISH improves the throughput, it is more suitable for RNA sequences with a length of 300–1500 nucleotides.[9] Therefore, it is significant to explore new strategies for monitoring the expression level of miRNA and visualizing their dynamic fluctuation within the context of intact living cells or tissues.

DNA molecules are pivotal biomolecules that responsible for storage and the transfer of genetic information in organisms, as well as, highly programmable molecular scaffolds for the fabrication of various nanostructures with well-defined form and precisely arranged device.[10] Given their biosecurity, addressability, and versatility, DNA-based nanosystem have become the robust tools to carry out various tasks in vivo, such as, biomolecular imaging, cargo transport, and release.[11] The past decade has witnessed ongoing process in DNA-based nanoprobes. Their basic task is to facilitate detection of a tiny amount of biomolecules through the generation of a measurable output signal.[12] To design the nanoprobes for intracellular miRNA detection and biological imaging, they must contain three basic components: a carrier, a receptor, and a transducer. In common, the carrier has a delivery function, which can facilitate nanoprobe sequences to enter the cells. The receptor for specific miRNA recognition is DNA sequence, that relies on A:U and C:G base pairing principle for preferential capture of target miRNA and resolving recognition event. The transducer is responsible for converting the biorecognition event into valid

F. Yang, H. Dong, X. Zhang
Marshall Laboratory of Biomedical Engineering Research Center for Biosensor and Nanotheranostic
School of Biomedical Engineering
Health Science Center
Shenzhen University
Guangdong 518060, P. R. China
E-mail: hfdong@szu.edu.cn

F. Yang
College of Basic Medical Sciences
Shanxi Medical University
Taiyuan 030001, P. R. China

F. Yang, H. Lu, X. Meng, H. Dong
School of Chemistry & Biological Engineering
University of Science & Technology Beijing
Beijing 100083, P. R. China

The ORCID identification number(s) for the author(s) of this article can be found under https://doi.org/10.1002/smll.202106281.

**DOI: 10.1002/smll.202106281**

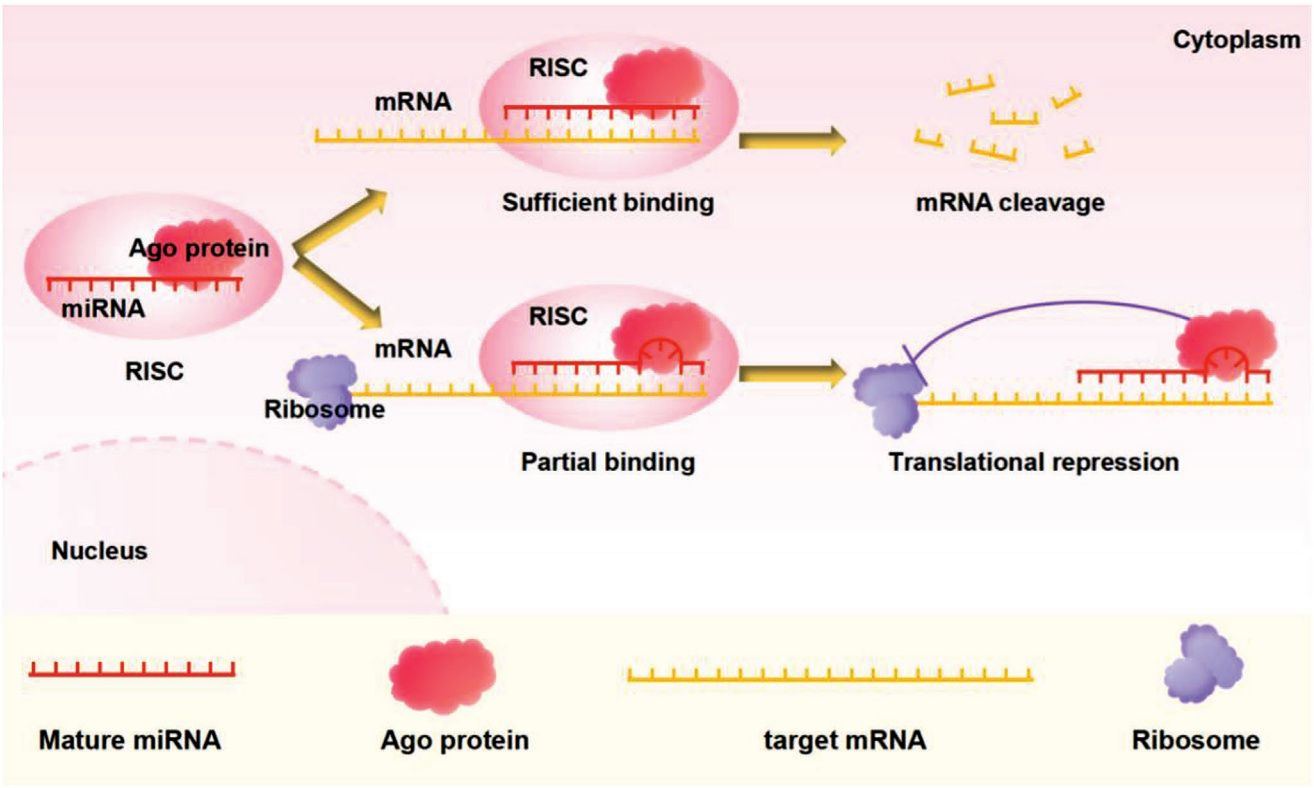


**Figure 1.** Schematic diagram of miRNA-induced gene regulation mechanisms.

signals, such as, optical and mechanical signals (**Figure 2**). In this review, we introduce delivery vehicles, sequence designs, and imaging technologies of nanoprobes, aiming to reveal how to design nanoprobes with desired properties for miRNA live-cell analysis. Finally, the outstanding challenges and future directions in the field are discussed.

## 2. Probe Delivery

During the cell journey, the first obstacle for the DNA probe sequence is the cell membrane that protect the cells from their surrounding environment.[16] It not only serves as a boundary to provide the structural support and maintain homeostasis, but also mediate the exchange of physical and chemical information between the cell and its environment.[17] As the exogenous genes, the DNA probe sequences cannot freely traverse the cell membrane due to their electronegativity and hydrophobicity. To solve the problem, paraformaldehyde and alcohol are generally used to pretreat the cells to enhance membrane permeability.[18] However, they may destroy the cell morphology and induce the cells death, leading the loss of the significance information for further research. Various of delivery vehicles have been developed to transport nanoprobes into cells.[19] In the section, we systemically introduce these nanoprobe carriers, including frame nucleic acids (FNAs), organic/inorganic nanomaterials, and lipid/cell membranes. The carrier-free intracellular delivery manner is also described. Their merit and demerit are summarized in **Table 1**.

### 2.1. Carrier-Assisted Intracellular Delivery

#### *2.1.1. Programmatic Frame Nucleic Acids as Delivery Vehicles*

The structural DNA nanotechnology has been rapidly developed from natural immobile Holliday junction to artificial FNAs, which shed a new light on spatially controllable patterning of functional biomolecules and biomaterials in vitro and in vivo.[10b,20] Various versatile FNAs have been explored as delivery platforms for biosensor.[21] They show distinct and unique superiorities including intrinsic biocompatibility and high internalized efficiency.[22] For example, Huang's et al had reported that DNA tetrahedral structure showed much higher cellular uptake ability than free single strand DNA.[23] Turberfield's group had proved a substantial uptake of tetrahedra into cells without other transfection agent.[24]

Furthermore, the FNAs showed good protection to the nanoprobes against nuclease degradation and protein interference. Dong et al. proved that DNA triangular prism could protect the hairpin probe from protein interference and DNase I degradation during the delivery process.[25] Zhang et al constructed a DNA nanocage with encapsulated nanoprobes for specific recognition and response target molecules. It was accessible to small miRNA, while large endogenous nuclease and non-specific proteins was blocked outside the cage, leading to a better anti-degradation and anti-interference ability than the probes attached to the outside FNA.[26] Importantly, the DNA nanocage showed a size-dependent protection effect.

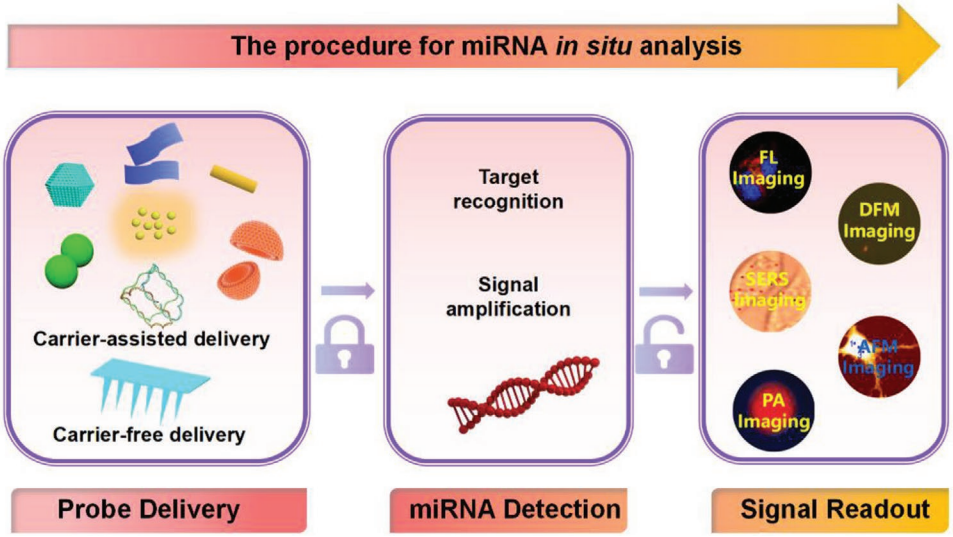


**Figure 2.** Schematic diagram of the procedure for miRNA in situ analysis. The imaging signals include fluorescence imaging (FL imaging), surface enhanced Raman spectroscopy (SERS) imaging, photoacoustic imaging (PA imaging), dark field microscopy imaging (DFM imaging), as well as, atomic force microscopy imaging (AFM imaging). SERS image is reproduced with permission.[13] Copyright 2017, American Chemical Society. PA image is reproduced with permission.[14] Copyright 2019, Wiley-VCH. AFM image is reproduced with permission.[15] Copyright 2018, American Chemical Society.

Additionally, the DNA intrinsic tailorable functionalities endow FNAs with excellent chemical addressability such as, DNA polyhedron,[22a,27] origami,[28] hydrogel structures,[29] micelles,[30] et al. The precision assembly and the high-ordered conformation of FNA make it a perfect template to organize various nanoscale molecules, such as proteins[31] and nanoparticles (NPs).[32] For example, Liu et al. constructed a DNA nanomachine (DNM) by alternately hybridizing two pairs of DNA/RNA hybrids to a DNA scaffold. The DNA cascade replacement reaction of DNA/RNA hybridization along the DNA scaffold was initiated by specific miRNA, triggering in situ assembly of siRNA sequences for gene therapy in vivo. (**Figure 3**A).[33] Kuang et al. fabricated a multifunctional nanopyramids by rational selection assembly of upconversion NPs (UCNPs), silver sulfide ($Ag_2S$) NPs, and Au-$Cu_9S_5$ NPs via DNA frame, that realize dual miRNAs bioimaging in living cells and a tumor-bearing mice (Figure 3B).[34]

There are several demerits of FNAs in live-cell analysis. For example, they show a poor specific recognition ability to cells, that usually need modify molecules (aptamer, peptides, and folic acids) to enhanced accumulation at target sites. Moreover, they exhibited inherent low load capability than organic/inorganic nanomaterials-based carriers due to limited functional sites on their surface.

**Table 1.** Comparisons of probe sequences delivery manners.

| Delivery manners | Merits | Demerits | Improvements |
|---|---|---|---|
| FNAs | Superior biocompatibility<br>High internalized efficiency<br>Good protection to probe sequences<br>Excellent addressability | Poor target ability<br>Low load capability | Modify molecules (aptamer, peptides, folic acids) to enhance target ability |
| Organic/<br>Inorganic nanomaterials | Mighty load capacity<br>Superior protection to probe sequences<br>Controllable release probe sequences | Potential cytotoxicity<br>Poor biocompatibility<br>Poor target ability | Modify molecules (PEG, aptamer, peptides, folic acids.) to reduce cytotoxicity, enhance biocompatibility and target ability |
| Liposomes | Good biocompatibility<br>Simple operation<br>High internalized efficiency for sophisticated system. | Poor target ability | Modify lipid surface (hyaluronic acid) to enhance target ability |
| Cell membranes | Superior biocompatibility<br>Low cytotoxicity<br>Homotypic target ability | Complicated operation | Simplified operation |
| Nanoneedle arrays | Superior transfection efficiency | Complicated operation | Simplified operation |

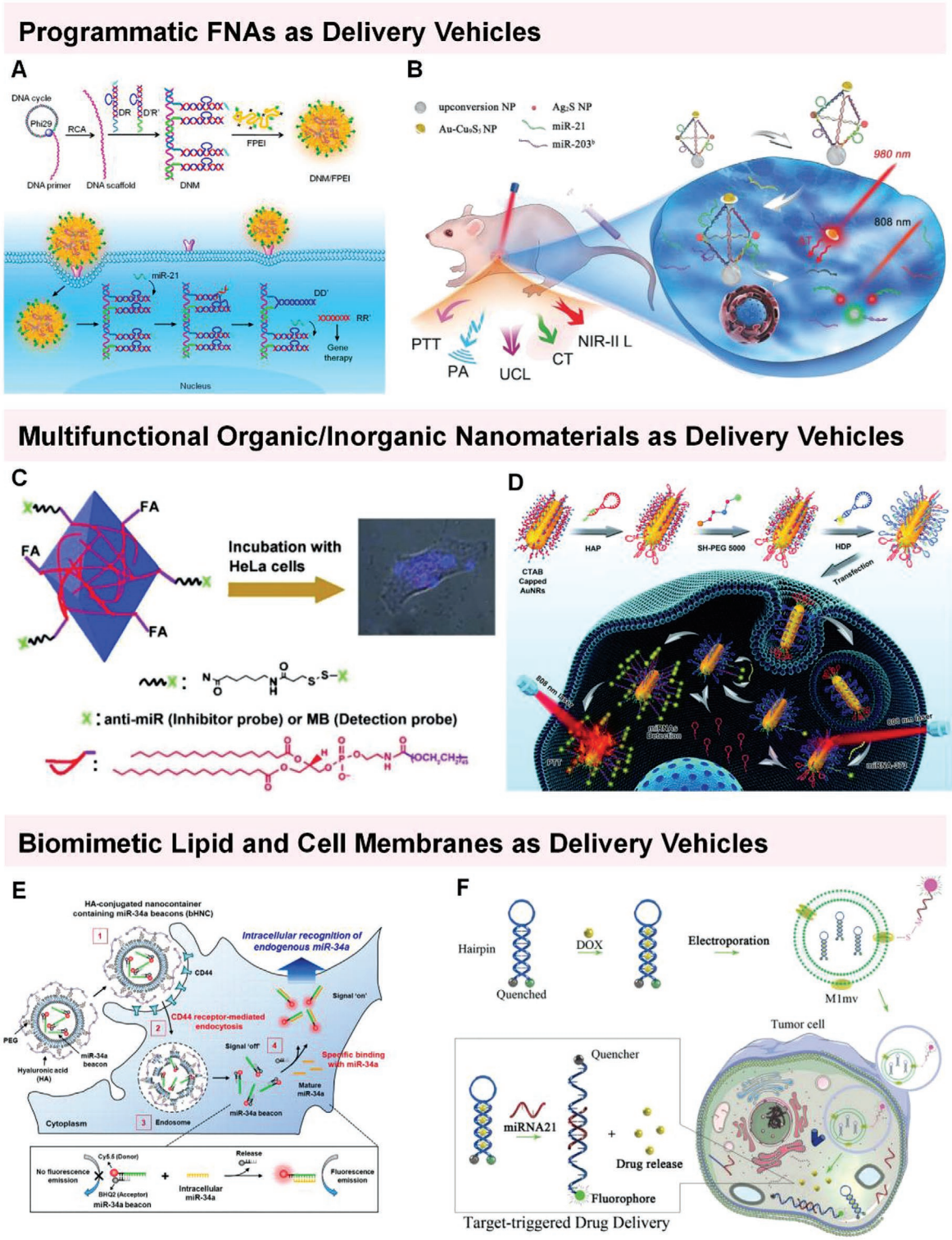


**Figure 3.** Carrier-assisted intracellular delivery. A) The miRNA-triggered DNM for intracellular siRNA cascade assemble in living cells. Reproduced with permission.[33] Copyright 2018, American Chemical Society. B) Nanopyramids for dual miRNAs detection and bioimaging in vivo. Reproduced with permission.[34] Copyright 2017, Wiley-VCH. C) The multifunctional $SnO_2$ nanoprobe for specific intracellular miRNA imaging. Reproduced with permission.[35] Copyright 2012, Wiley-VCH. D) Near-infrared triggered strand displacement amplification for miRNA quantitative detection in single living cell. Reproduced with permission.[36] Copyright 2018, The Royal Society of Chemistry. E) Target miR-34a beacon delivery system based on HA-coated nanocontainers for targeted intracellular recognition of miR-34a. Reproduced with permission.[37] Copyright 2012, American Chemical Society. F) Target-triggered drug delivery system based on M1mv–DNA–QDs. Reproduced with permission.[38] Copyright 2019, Wiley-VCH.

#### 2.1.2. Multifunctional Organic/Inorganic Nanomaterials as Delivery Vehicles

Various organic and inorganic nanomaterials have attracted intensive interest to construct nanoprobes delivery vehicles due to their unique and intriguing properties.[11a,39] Generally, the surface of the nanomaterials is required to be modified with different molecules such as PEG, aptamer, peptides, folic acids, et al. to reduce potential cytotoxicity, to acquire desirable biocompatibility and target capability.[40] These nanomaterials show a mighty load capacity to nanoprobes via physical entrapment or chemical conjugation including electrostatic interactions, $\pi$-$\pi$ stacking, hydrogen bonding interaction and classic chemical reaction (**Table 2**) owing to the flexibility to function. The nanomaterials vectors can provide sufficient protection to the nanoprobes under physiological conditions.[41] For example, Wang et al. reported that the split-DNAzyme probe loaded on Au NPs showed negligible degradation after DNase I treatment for 1 h.[42] Huo et al. demonstrated that zeolitic imidazolate framework-8 (ZIF-8) NPs could protect nanoprobes from DNase I degradation.[43] Ju et al. designed multifunctional $SnO_2$ NPs as efficient delivery vector, which showed good protection to molecular beacon (MB) probe from nucleases and interfering proteins (Figure 3C).[35] The protection may be resulted from the steric shielding of the nanomaterials and the conformational change of nucleic acid strands.

Controllable release of probe sequences is significant for intracellular miRNA spatiotemporal detection. The photothermal effect of nanomaterials vectors are reported to deliver nanoprobe into cells and controllably activate signal amplification to realize miRNA imaging with high sensitivity. Dong et al. functionalized two types of programmable oligonucleotide hairpin probes, named as hairpin assistant probe (HAP) and dye-labeled hairpin detection probe on the terminal and side surfaces of Au nanorods (THP-AuNRs) for sensitive intracellular miRNAs detection, respectively.[36] The external near-infrared (NIR) triggered HAP release and strand displacement amplification for miRNA detection in single living cells or in multicellular tumor spheroids (Figure 3D). Furthermore, his group designed hollow copper sulfide NPs as carriers and photothermal conversion agent to carry entropy-driven toehold-mediated strand displacement reaction, that realized miRNA triggered catalytic imaging without additional transfection of fuel DNA strand.[62]

#### 2.1.3. Biomimetic Lipid and Cell Membranes as Delivery Vehicles

Cationic liposomes are robust candidates as nucleic acids transfection reagents that show significant biocompatibility, biodegradability, biosecurity, controllable size, and surface manipulations.[11b,63] They form complexes with nucleic acids to neutralize the negative charge of nucleic acids and weaken the electrostatic repulsion to the cell membrane.[64] The commercially produced cationic liposomes, such as lipofectamine, supply a convenience for probe sequences delivery since they are simple to operation, cost-effective

**Table 2.** Summarized representative nanomaterials as delivery vehicles of probe sequences.

| Nanomaterials | Interaction | Surface modification | Ref. |
|---|---|---|---|
| $MnO_2$ nanotubes | Van der Waals force (Electrostatic interaction) | | [44] |
| g-$C_3N_4$ nanosheet | $\pi$–$\pi$ interaction | | [45] |
| $MoS_2$ nanosheet | Van der Waals force | | [46] |
| $MnO_2$ nanosheet | Van der Waals force | | [47] |
| $WSe_2$ nanosheet | Electrostatic interaction and $\pi$–$\pi$ interaction | Surface perfluorination | [48] |
| Carbon nitride nanosheet | $\pi$–$\pi$ interaction | Folate (FA)-Poly A | [49] |
| Hexagonal boron nitride nanosheets | $\pi$–$\pi$ interaction | | [50] |
| Graphene oxide nanosheet | $\pi$–$\pi$ interaction | | [51] |
| $MoS_2$ QDs | Van der Waals force | | [52] |
| SiC QDs | Van der Waals force | PEG | [53] |
| Graphene QDs | Specific adsorption and $\pi$–$\pi$ interaction | PEG and polylactic acid | [54] |
| $SnO_2$ NPs | Van der Waals force and hydrophobic interactions | DL-PEG2000-FA and DL-$PEG_{2000}$-SPDP-MB | [35] |
| Au@PDA NPs | $\pi$–$\pi$ interaction and hydrogen bonding | | [55] |
| UCNP | Electrostatic interaction | Cationic polymer (poly-lysine) | [56] |
| Dendritic mesoporous silica nanoparticles (DMSNs) | Disulfde bond (—S—S—) | —SH | [15] |
| ZIF-8 NPs | Electrostatic interaction | | [57] |
| Gold-nanodot-decorated hollow carbon nanospheres (AuHCNs), | Specific adsorption and $\pi$–$\pi$ interaction | Hyaluronic acid (HA) | [58] |
| Au NPs and Au NDs | Au—S bond | | [59] |
| Au NRs | Electrostatic interaction | PEI-SH | [60] |
| Au nanocages | Au—S bond | BSA | [61] |

and high-performance for sophisticated detection systems. For instance, Wang et al. developed a proteinase-free and nanomaterials-free replicated hybridization chain reaction (R-HCR) machinery using the cross-invasion of HCR and DNAzyme catalysis for miRNA detection.[65] Lipofectamine 3000 reagent was used as delivery vehicle to transfect R-HCR system into cells and living mice for imaging miRNA with good performance. Wu et al. developed a branched DNA junction-enhanced isothermal circular strand displacement polymerization (B-ICSDP) for intracellular miRNAs imaging using Lipofectamine 2000 transfection.[66] To enhance the cell targeting ability, Haam et al. constructed hyaluronic acid (HA) coated liposome nanocontainers containing simple miRNA-34a beacons (bHNCs). It enabled target-cell-specific transfection of metastatic breast cancer cells with up-regulated cell surface adhesion molecule cluster determinant 44 (CD44) through HA affinity to CD44 and intracellular recognition of miRNA-34a (Figure 3E).[37]

Recently, cell membrane vesicles have emerged as powerful delivery tools. Besides superior biocompatibility and low cytotoxicity, they show fascinating ability to target homotypic cells. Huang et al. constructed an engineered artificial vesicle of M1 macrophages (M1mv) via a pneumatic liposome extruder with tumor cells killing capacity (Figure 3F). The hairpin DNA fluorescence quantum dots (QDs)-labeled probes intercalated by DOX were loaded in M1mv (M1mv–DNA–QDs), which entered cells through electroporation, and the hairpin probe could be recognized by miRNA and release DOX for therapy.[38] The application of cell membrane vesicles-based carrier is limited by complex procedure for cell membrane preparation. Simplified operation could compensate the drawback of cell membrane.

### 2.2. Carrier-Assisted Intracellular Delivery

Recently, the nanoneedle arrays have been developed as minimally invasive tools for in situ probing specific signaling transduction and detecting biomolecular in living cells since their superior transfection efficiency. The technique relies on controlled force that nanoneedle arrays can temporarily puncture the cell membrane and induced its deformation via a well-controlled centrifugation facilitated procedure.[67] At the same time, the exogenous materials can diffuse into cell cytosol before the recovery of the membrane deformation. Shi et al. had applied the nanoneedle arrays for delivering plasmid DNAs into neurons, the carrier-free intracellular delivery improved at least eightfold in transfection efficiency compared to the lipofection transfection approach.[68] Furthermore, they used the diamond nanoneedles to deliver probe which hybridized with target miRNA and directly isolated the double-strand RNA product via RNA binging proteins from cytoplasm while keeping the cells alive.[69] Afterward, the miRNA signal was amplified via HCR. They proved that the in situ profiling approach could decipher spatial dynamic information regarding the cells by quantifying the relative distribution of the diamond nanoneedles with miRNA signals. The demerit of nanoneedle arrays-based delivery manner is complicated operation procedure. Simplified operation may compensate the drawback of nanoneedle.

## 3. Probe Sequence Design

The probe sequences are responsible for miRNA capture and resolving procedure, which endow biosensor the ability of selectivity and sensitivity. The specific miRNA recognition event mainly relays on A:U and C:G base pairing principle, which probes sequences are preferential complementary to a target miRNA. In the absence of target miRNA, the probes act as signal locks to avoid premature signal leakage. The switches that initiate the hybridization between target miRNA and probe sequences are fallen into two broad categories: the one is an extended single stranded region known as toehold. Another is the loop of hairpin structure. All these structures are key factors to enhance specific selection of probe sequences. Equally important is the sensitivity since "one-to-one" signal output could not satisfy the low-abundance miRNA detection in the cells. Various exquisite cascade reactions are emerging as attractive candidates for signal amplification, such as, catalytic hairpin assembled reaction, HCR, and DNAzyme-powered amplification reaction et al., which have been extensively explored and summarized. Furthermore, the self-calibration strategies, such as ratiometric signals, dual-signal output, also been exploited to avoid false positive signals during delivery procedure or system design defects. In the section, we will concentrate on other new design strategies of probe sequences for enhanced miRNA detection.

### 3.1. Photo-Controlled microRNA Biorecognition

Photo-controlled biorecognition refers to exogenous laser assisted detection system, which biorecognition sequence is protected during probe endocytosis process. After the probe reaches the cytoplasm, the biorecognition sequence is exposed with an external laser irradiation and initiator the miRNA biorecognition event. The spatial-temporal protection effectively avoids passive miRNA-probe interaction and false positive signals output, which is benefited for accurate biological analysis. For example, Li et al. designed a NIR light-activatable DNA nanodevice through integration the photocleavable (PC) bond inserted MBs with UCNPs that played as the NIR-to-ultraviolet (UV) transducers (**Figure 4**A).[56] The miRNA recognition function was blocked temporarily until a NIR light irradiation. Subsequently, the PC bonds were cleavage due to the photolysis, and the intracellular miRNA sensors were activated. The feasibility of nanodevice had been validated for intracellular spatiotemporally control miRNAs sensing and imaging, even expanded to an activatable imaging of intra-tumoral miRNAs in living mice. Moreover, they developed a triphenylphosphonium-functionalized DNA nanoreporter technology for two types of cancer-related mitochondrial miRNAs imaging in live cells, which kept silence during delivery process and was photoactivated after targeted mitochondrial localization

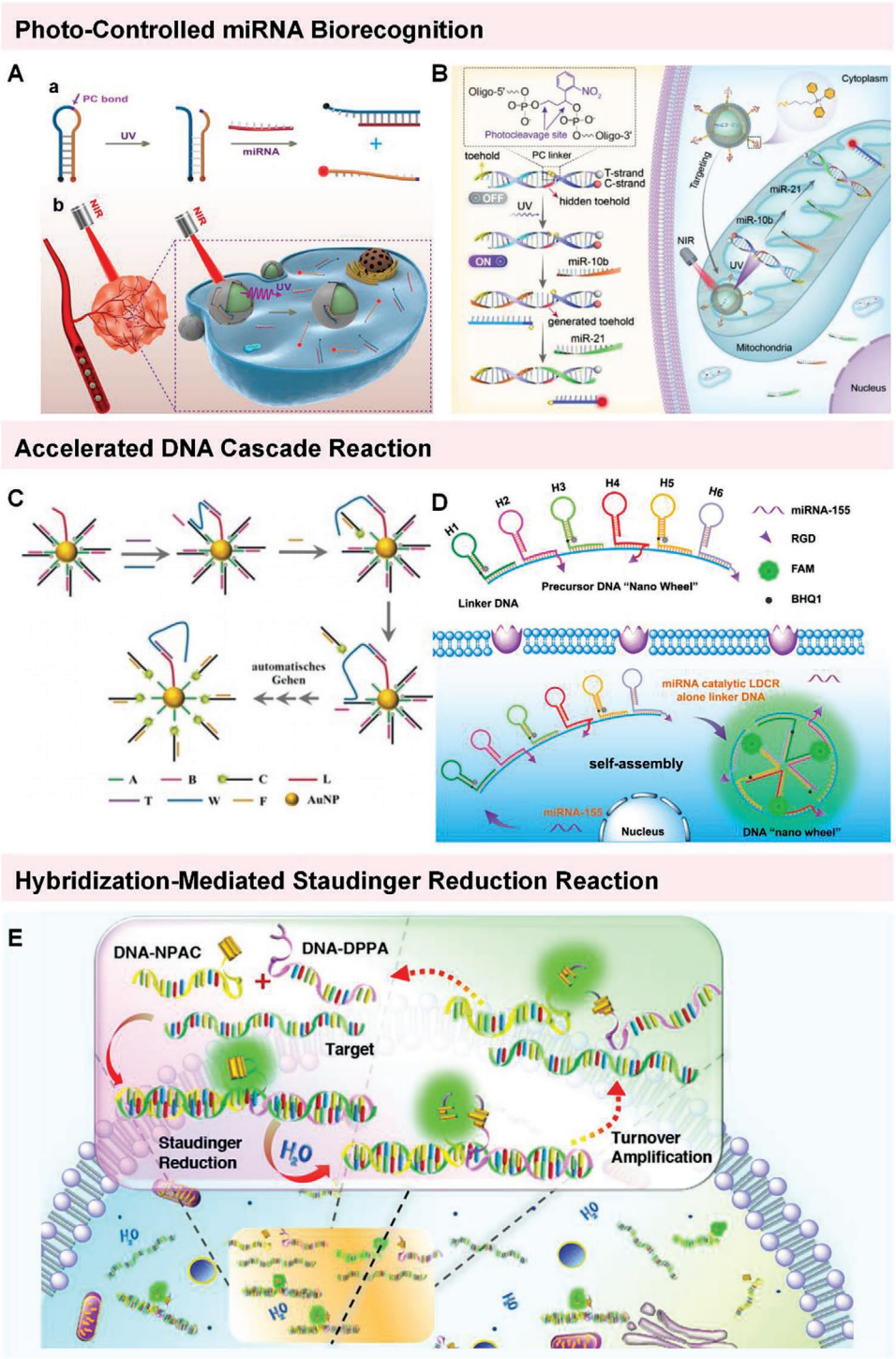


**Figure 4.** Probe sequence design. A) The activatable DNA nanodevice for NIR light-controlled miRNA sensing and imaging. Reproduced with permission.[56] Copyright 2019, American Chemical Society. B) The DNA nanoreporter technology for imaging of mitochondrial miRNAs via NIR light-controlled strand displacement reactions. Reproduced with permission.[70] Copyright 2021, Wiley-VCH. C) Entropy-driven DNA nanomachine for miRNAs analysis. Reproduced with permission.[71] Copyright 2017, Wiley-VCH. D) MiRNA-triggered localized DNA cascade reaction alone the linker DNA for visualization of miRNA in situ. Reproduced with permission.[72] Copyright 2019, American Chemical Society. E) The functional hybridization-mediated Staudinger amplification reduction reaction for miRNA detection. Reproduced with permission.[73] Copyright 2019, American Chemical Society.

(Figure 4B).[70] The technology allowed precise control over miRNA imaging at subcellular level, which provided a robust tool for investigating mitochondrial miRNA-associated physiological events.

### 3.2. Accelerated DNA Cascade Reaction

Accelerated target analyte response or shorten the reaction time can effectively reduce endogenous interference on the probes and improve the detection sensivity. In a homogeneous solution, the intermolecular reaction between analyte molecules and nucleic acid probes depends on the diffusion of the random spontaneous collision in a typical 3D fluidic space, which extend reaction time and limit low-abundance miRNA detection. Localized concentration amplification via integrating the probes on the surface of NPs or FNAs, has been proposed by researchers that could increase effective collisions. Based on the principle, Yin and co-workers tailored an elegant entropy-driven DNM with predictable and automatic 3D detection track for intracellular miRNA imaging.[71] As showed in Figure 4C, the target (T) enables to tether a walking leg (W) strand to the Au NPs surface via hybridization with affinity ligand (L), which initiated the entropy-driven catalytic reaction of intramolecular toehold-mediated strand migration. The DNM displaced enhanced sensitivity and reaction kinetics than conventional Au NP-based intermolecular reaction, attributed to motion components co-anchored on a single Au NP resulting in enhanced local effective concentrations. Dong and co-workers anchored 6 DNA hairpin structures on a DNA nanowire for intracellular miRNA-155 imaging via localized DNA cascade reaction. When the miRNA-155 activated the system, the hybridization reaction occurred from hairpin H1 to H6 to form a DNA "nano wheel" structure (Figure 4D).[72] The system was superior to miRNA-triggered 6 free hairpin monomers without fixed on DNA nanowires in reaction kinetics and sensitivity since the local effective concentrations of each DNA hairpin probe was increased by 2748-fold.

### 3.3. Hybridization-Mediated Staudinger Reduction Reaction

Different from conventional stand-displacement mediated amplification reaction, Peng and co-worker first applied hybridization-mediated Staudinger reduction (HMSR) to design a fluorogenic response strategy for miRNA detection.[73] As shown in Figure 4E, the HMSR-probe was consisted with 1,8-naphthalimide derivative (DNA-NPAC) and 3-(diphenylphosphino) propionic acid (DNA-DPPA) to recognize and hybridize with target miRNA. It would confine the reactive site of azido group and diphenylphosphino molecule into proximity in a compact space, leading to the fluorescence recovery of the naphthalimide fluorophore. More important, it resulted in the separation of HMSR-probe in physiological environment due to the presence of $H_2O$ in the Staudinger system, accompanied by miRNA re-release and recycle. As bio-orthogonal "click reaction," the Staudinger reduction for miRNA detection was compared with azide–alkyne cycloaddition (CuAAC) reaction, which showed an ameliorative detection limit and higher sensitivity. The HMSR-probes were applied for miRNA-24 analysis in living cells, mice tissues slice, and clinical patient serum samples. Note that the fluorescence intensity in serum samples of pancreatic cancer patients showed a significant enhancement than that in the serum sample of pancreatitis and healthy people. Meanwhile, a negligible difference among the samples from both patients with pancreatitis and healthy people has been found for a quite low concentration of target miRNA. The same trend of signal change among different stages of pancreatic disease also was observed by conventional qRT-PCR strategy. Taken together, the exquisite fluorogenic response system could serve as a robust and reliable tool for miRNA analysis in clinical samples and supply a new idea for the design of hybridization amplification reaction.

## 4. Imaging Signals

Various imaging analysis technologies have offered noninvasive tools for intracellular signal readout and lighting morphological details of cells/tissues or mapping the endogenous gene expression with subcellular resolution and high detection sensitivity.[74] In this section, we will discuss recently developed intracellular miRNA imaging signal detection and output technologies including the fluorescence imaging (FL imaging), surface enhanced Raman spectroscopy (SERS) imaging, photoacoustic imaging (PA imaging), dark field microscopy imaging (DFM imaging), as well as, atomic force microscopy imaging (AFM imaging)

### 4.1. Fluorescence Imaging

Fluorescence is a cold photoluminescence phenomenon that light emission accompanied by radiative relaxation when the substance in an excited state returns to its ground state.[74a] Fluorescence imaging technology has become one of the most powerful and reliable tool for direct visualization spatial distribution and monitoring temporal fluctuation of analyte concentration in cellular microenvironment.[75] Various fluorescent agents including organic molecules, fluorescent proteins, fluorescent NPs et al. have been reported for constructing intracellular miRNA analysis system.

The organic fluorescence dyes have been widely used as the reporting signals for probe since the amenability to DNA sequence modification. The conjugation organic fluorescence dyes to any position of DNA sequence are facile and commercially available, which facilitate to nanoprobes design, especially in complex and multiple detection systems. For example, Dong et al. utilized FAM, Cy3, and Cy5 as fluorescence dyes to label different nanoprobe, realizing simultaneously and sensitively imaging three types of miRNAs in living cells (**Figure 5**A).[76] Wang et al. used FAM and Cy3 as fluorophores pairs to produce a tremendously amplified fluorescence resonance energy transfer signals for intracellular miRNA-21 detection.[77]

Fluorescent proteins are highly attractive as fluorescent labels in the biological field, which allow specific cellular or viral protein to be labeled by genetic engineering.[75] Jiang et al. designed a genetically encoded light-up RNA sensor for intracellular miRNA fluorescence imaging using green fluorescent protein (GFP) co-expression as internal reference.[78] After transfection into the cells, the RNA sensor output an orange fluorescence signal in response to target miRNA-21, whereas the GFP gave target-independent green fluorescence

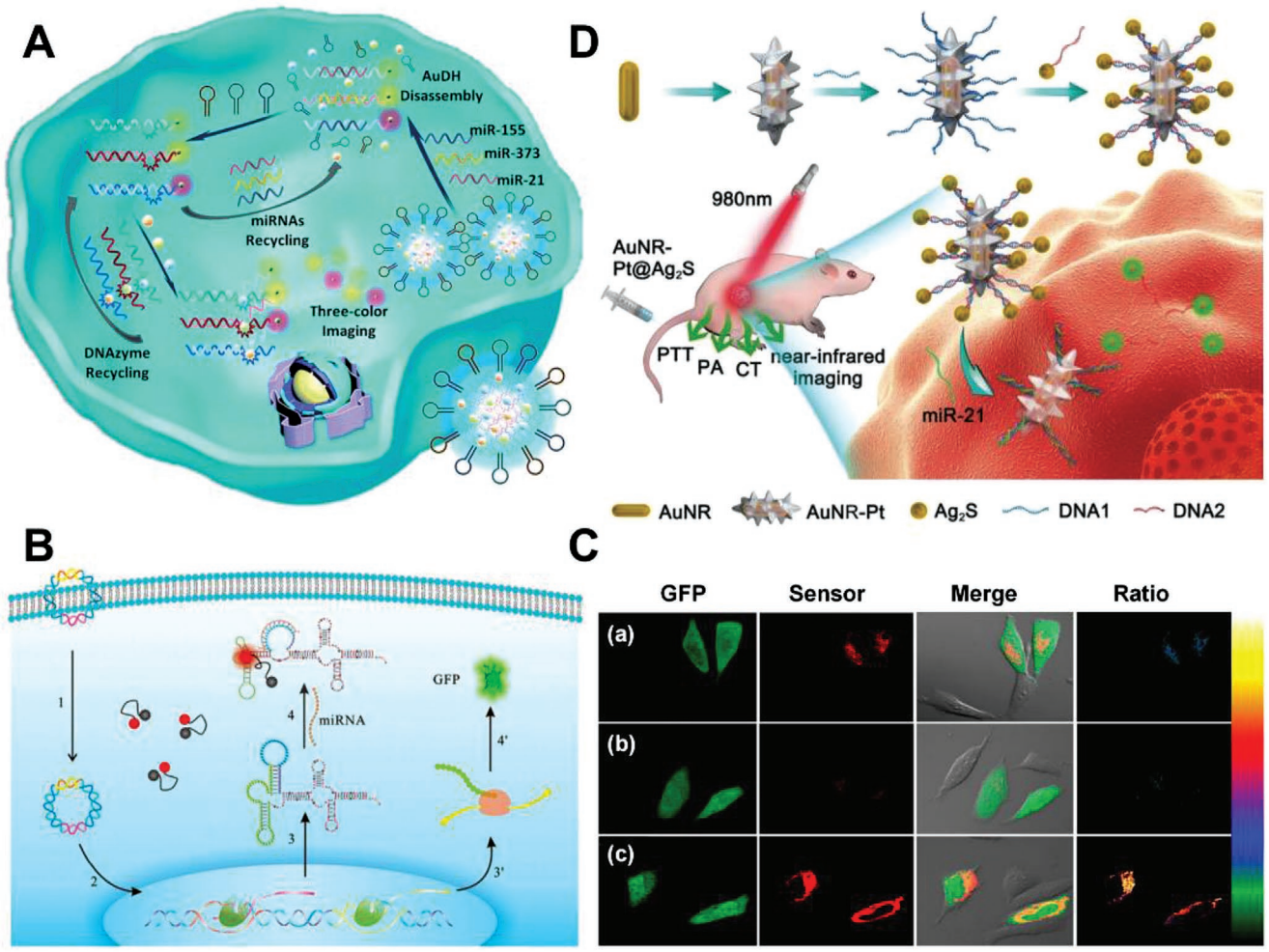


**Figure 5.** Fluorescence imaging for intracellular miRNA detection. A) DNA-capped-Au assembled hydrogels for imaging of multiplex miRNAs. Reproduced with permission.[76] Copyright 2018, The Royal Society of Chemistry. B) The genetically encoded RNA sensor for ratiometric miRNA imaging and C) fluorescence imaging for Hela cells (a: control; b: treated with 300 nM miRNA inhibitor; c: treated with 300 nM miRNA mimic). Reproduced with permission.[78] Copyright 2017, American Chemical Society. D) Photoactive hybrid AuNR-Pt and $Ag_2S$ core–satellite assembly for miRNA-21 detection and multimodal imaging guided photothermal therapy. Reproduced with permission.[79] Copyright 2017, Wiley-VCH.

as an internal reference (Figure 5B). The red fluorescence showed different intensities due to up-regulation or down-regulation of miRNA-21, while the bright and uniform distribution of green fluorescence signals in the nuclei and cytosol afforded an ideal internal standard signal for ratiometric imaging. The design provided a new paradigm for developing sensitive light-up RNA sensors for miRNA imaging applications.

As alternative to fluorescent dye or protein, QDs possesses superior optical properties including high quantum yield, long lifetime, excellent photostability, broad absorption, and narrow tunable emission, holding great promise for fluorescent labels.[80] The bioconjugates of QD and DNA molecular probes are extensively applied for miRNA imaging in vivo.[81] For example, Ma et al. designed a DNA-templated Au NP–QD assembly probes for high-sensitive catalytic imaging of miRNA in living cells.[82] The $Ag_2S$ QDs with the NIR window fluorescence signal were reported for the ultrasensitive and selective detection of miRNA in cells and solid tumors of mice with lower autofluorescence, reduced photon scattering, deeper tissue penetrations (Figure 5C).[79]

UCNPs-based nanoprobes are intriguing imaging tools that exhibit significant feature to avoid autofluorescence interference due to typical anti-Stokes luminescence principle.[74b] Kuang et al. used UCNP to construct luminescence resonance energy transfer (LRET) miRNA biosensing platform.[83] The core-satellite superstructures were constructed using DNA as bridge to assemble UCNPs, Au NRs, and dye molecules (TAMRA and Cy5.5). The luminescence of UCNP was largely quenched due to the LRET to Au NRs under a 980-nm laser excitation. After target miRNAs recognition, the TAMRA dye (588 nm) and Cy5.5 (736 nm) were lighted up due to the dissociation of UCNPs from the ends. It affords Zeptomolar sensitivity to simultaneous imaging of two miRNA markers in living cells and in vivo. Bi et al. designed a LRET-based upconversion nano-sensor using dual dyes (TAMRA and BHQ1 modified on cDNA) as acceptors to enhance quenching efficiency, realizing a low background signal and a high sensitivity for miRNA-21 imaging in living cells.[84]

### 4.2. Raman Imaging

The Raman effect was originally applied to identify bonds and molecules by measuring the magnitude of energy loss of inelastically scattered photons to ascertain their vibrational modes.[74a] Raman signal is intrinsically quite weak since only about one in a million photons scatters inelastically when the photons pass through a material.[85] SERS effect refers to the Raman signal of the Raman molecule is greatly enhanced when it is confined on the plasmonic metal (e.g., Cu, Ag, and Au) surface or located in the nanogap of plasmonic metal nanostructures because of the enhanced local electromagnetic fields generated nearby the metal NPs.[74a] SERS is an ultrasensitive vibrational spectroscopy technology and has drawn much attention

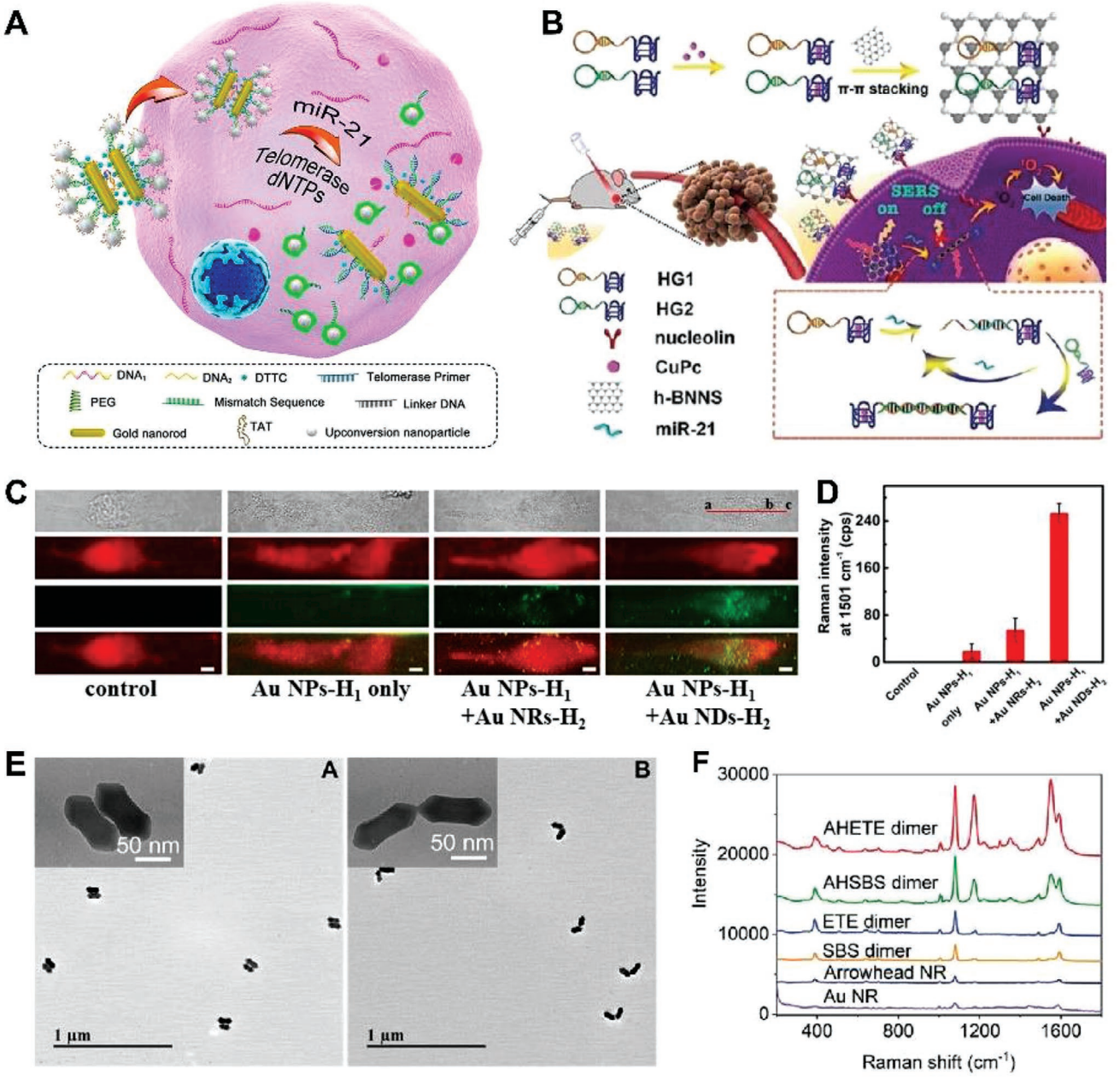


**Figure 6.** Raman imaging for intracellular miRNA detection. A) The Au NR Dimer-UCNP core–satellite nanostructures for the simultaneous analysis of intracellular miRNA-21 and telomerase. Reproduced with permission.[13] Copyright 2017, American Chemical Society. B) The multifunction CuPc@HG@BH theranostic platform for SERS real-time monitoring of miRNA and photodynamic therapy. Reproduced with permission.[50] Copyright 2019, Wiley-VCH. C) A549 cells were detected with Au NPs-H1 probes (0.18 nM) and Au NDs-H2 probes (0.021 nM), Au NPs-H1 probes (0.18 nM) and Au NRs-H2 probes (0.021 nM), or Au NPs-H1 probes (0.18 nM) only. D) Raman intensity at 1501 $cm^{-1}$ of A549 cells with different treatment in (C). Reproduced with permission.[59] Copyright 2018, American Chemical Society. E) TEM image of AHSBS dimer and AHETE dimer. F) Raman spectra of various dimer and single NRs. Reproduced with permission.[88] Copyright 2020, Wiley-VCH.

for versatile applications.[86] In comparison with fluorescence imaging, it shows better photostability to resist photodegradation and photobleaching.[74b] Importantly, its narrower spectral width to relieve the spectral peak overlapping problem between different signal molecules.[87]

Generally, the intelligent integration of nanocomposite can display good SERS effect. For example, Au NR dimers as SERS-based probes substrate was connected with UCNPs to form a core–satellite nanostructures for the simultaneous analysis of intracellular miRNA-21 and telomerase (**Figure 6**A).[13] The NRs with curvatures or sharp edges have better Raman enhancement ability to act as SERS substrate fabrication candidate. Dong et al. developed plasmonic Au (nanodumbbel) NDs as core and Au NPs as satellites that response to target miRNA to construct polamonic core-satellite probe (Au NPs-Au NDs) for miRNA SERS imaging in living cells. It possessed a significantly enhanced electromagnetic field and advanced SERS sensitivity than the system that Au nanorods as core and Au NPs as satellites (Au NPs-Au NRs) (Figure 6C,D).[59] Xu et al synthesized arrowhead Au NRs and assembled them end-by-end (known as AHETE dimers) and side-to-side (known as AHSBS dimers, Figure 6E). Compared to typical cylindrical Au NR dimers, the SERS reporter molecule 4-ATP on the surface of arrowhead NR dimers showed a stronger signal (Figure 6F), which was more suitable for miRNA nanoprobes.[88]

Besides plasmonic metal NPs, 2D nanomaterials have also been reported as promising SERS substrate.[89] Tian et al. developed a multifunctional integrated theragnostic nanoplatform using hexagonal boron nitride nanosheets (h-BNNS) as SERS substrate (Figure 6B).[50] The copper (II) phthalocyanine (CuPc) molecule was intercalated into hairpin G-quadruplex as SERS reporter molecule for miRNA detection and photosensitizer (PS) for photodynamic therapy. The SERS signals was significantly enhanced when it was conjugated on the h-BNNS attributed to the interface dipole interaction between h-BNNS and CuPc induced by the highly polar B—N bond and resulted symmetry-related perturbation in CuPc, achieving a limit of detection (LOD) as low as 0.7 fM in living cells. Kuang and co-workers designed a graphene oxide (GO)-gold-nanoparticle (Au NP) assemblies for simultaneously detection surface glycoprotein

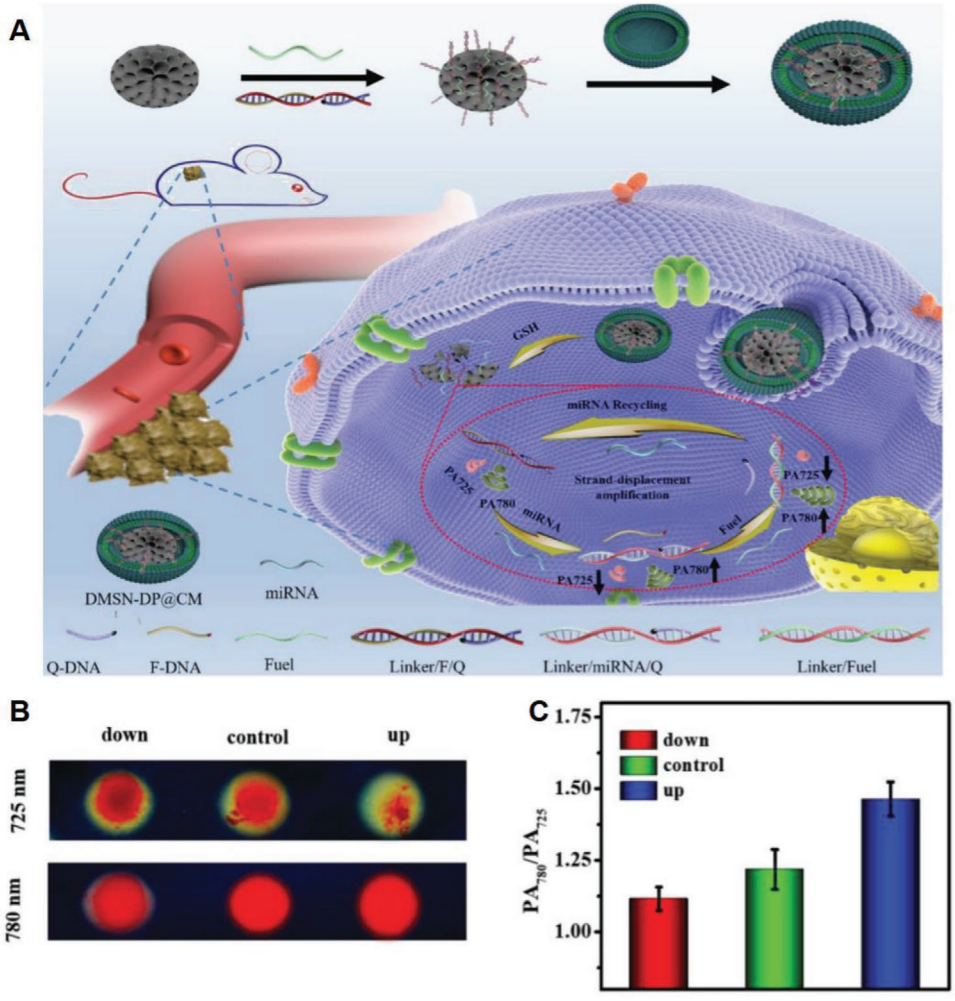


**Figure 7.** PA imaging for intracellular miRNA detection. A) Cancer cell membrane camouflaged nanoprobe for catalytic ratiometric photoacoustic imaging of miRNA in living mice. B) The PA imaging of mcf-7 cell treated with miRNA-21 inhibitors and miRNA mimics. C) The values of ratiometric PA signal at 780/725 nm correspond to the groups in (B). Reproduced with permission.[15] Copyright 2019, Wiley-VCH.

and miRNA in living cells.[90] When the miRNA was hybridized with a molecular probe, the FAM-modified Au NPs would separate from GO and result in a decrease in Raman signal. The strategy showed a linear range of 0.07–13.68 amol $ng^{-1}_{RNA}$ and LOD of 0.03 amol $ng^{-1}_{RNA}$.

### 4.3. Photoacoustic Imaging

Photoacoustic imaging (PA imaging) is an accurate noninvasive and nonionizing modality to visualize distribution of pathological biomarkers at the molecular level in vivo.[91] It harvests the advantages of both optical and acoustic imaging that utilizes short-pulsed light radiation as probing energy and collects ultrasound generated by photon absorption and thermoelastic expansion to generate images.[85,92] Due to low scattering of ultrasound in biological tissue, PA imaging can provide a deeper photoacoustic signal penetration into tissues (beyond the limit of the optical window) and a higher spatial resolution than other optical technologies.[74c,93]

Conventional photoacoustic probes utilize endogenous or exogenous light absorbers as entities to produce accumulated signals in targeted tissue. To satisfy the target analysis, activatable photoacoustic probes that combine molecular recognition module to produce modulated photoacoustic signals have been widely developed. Dong et al. developed a miRNA triggered photoacoustic nanoprobes that constructed by DNA sequences bound a NIR PA imaging pair (**Figure 7**A).[15] The system enables imaging miRNA-21 change in living cells with accuracy and fidelity (Figure 7B,C), which indicated its enormous potential in advanced molecular imaging in vivo. Tang et al. developed a self-assembled HCR PA nanoprobe, which realized highly sensitive assessment abundance changes of miRNA-155 during breast tumorigenesis and chemotherapy.[94]

### 4.4. Dark Field Imaging

Based on the unique and controllable Rayleigh light-scattering properties of plasmonic nanomaterials (PNMs), dark-field imaging (DF imaging) technology have provided a type of robust signal readout mode at the single-molecule level to monitor a serious of dynamic physiological processes, such as endogenous gene expression,[95] NPs internalization,[96] and subcellular movement.[97] Generally, the scattering signal of PNMs is very sensitive to their component, size, shape, refractive index of the surrounding environment, and the extent of plasmonic coupling.[74a,98] In addition, in comparison with

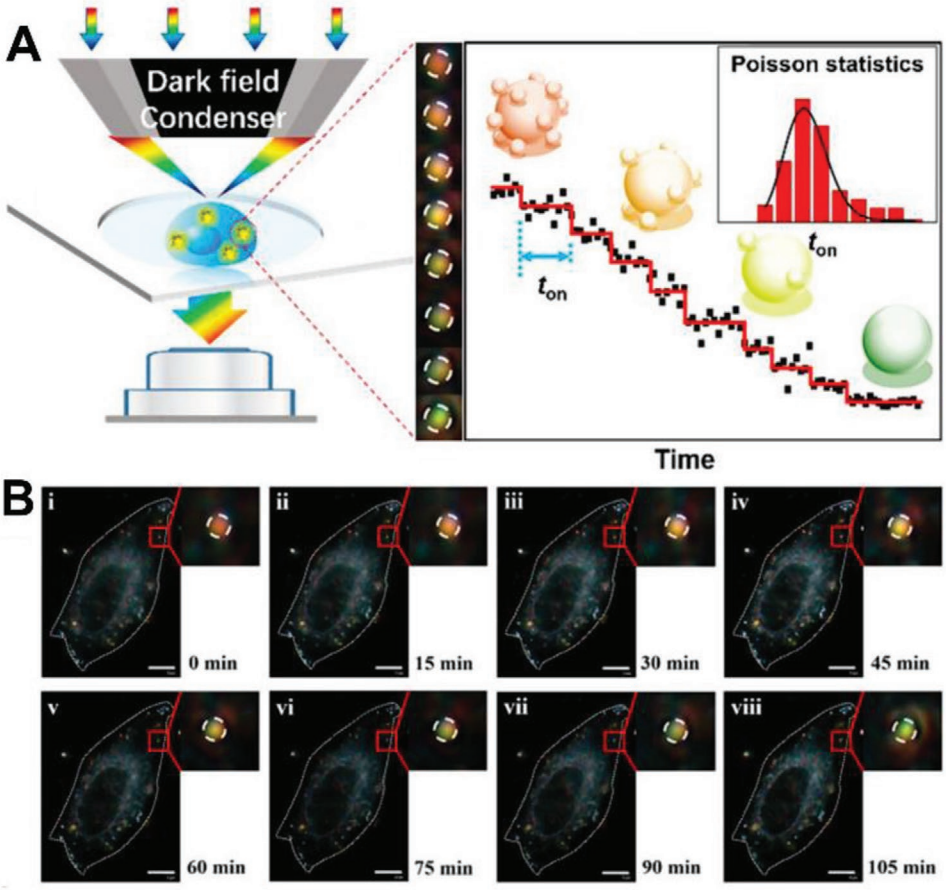


**Figure 8.** Dark-field imaging for intracellular miRNA detection. A) The detection principle of plasmon rulers induced by miRNA. B) Continuously imaging of single living HeLa cell after the introduction of plasmon rulers. Scale bars: 10 μm. Reproduced with permission.[102] Copyright 2018, American Chemical Society.

fluorophore-based single-molecule-level imaging and analysis methods, which suffer from the blinking and bleaching problems of fluorophores, the DFI greatly extend the observation time for monitoring biological processes in living cells.[99] Therefore, DFI technology have received considerable attention for intracellular single-molecule imaging.

With the aid of dark field microscope (DFM), plasmon ruler, a core-satellite multimer of PNM linked by polymer, such as, DNA,[100] peptides,[101] have been demonstrated to act as efficient dynamic molecular rulers. In these systems, the single-molecule recognition event could be transformed into color change, which can be directly captured by a commercial color camera and analyzed by RGB channels of color image. For example, Xu et.al. had utilized it for quantitative detection of miRNA-21 in living cells.[102] It was proved that the distribution of the time range for single strand displacement event was target miRNA concentration-dependent, which obeyed Poisson statistics (**Figure 8**A). The concentration of miRNA-21 in Hela cells was calculated to be around 2.14 nM according to the statistical analysis (Figure 8B).

### 4.5. Atomic Force Microscopy Imaging

The atomic force microscope (AFM) has been explored for investigating biomolecular interactions at the single cell level.[103] Briefly, the nanoscale distribution of the target molecule can be visualized by tracking the force–distance (*F–D*) curve within the relevant interval in force mapping mode.[104] Kim and his co-workers had used a hybrid binding domain (HBD)-tethered AFM tips technology to directly and sensitively visualized and quantified miRNA in a single cell.[14] As shown in **Figure 9**A, the HBD was an N-terminal domain of human RNase H1 could bind to the minor groove of RNA/DNA hybrid duplex structure in a sequence-independent pattern. The technology realized in situ resolve individual

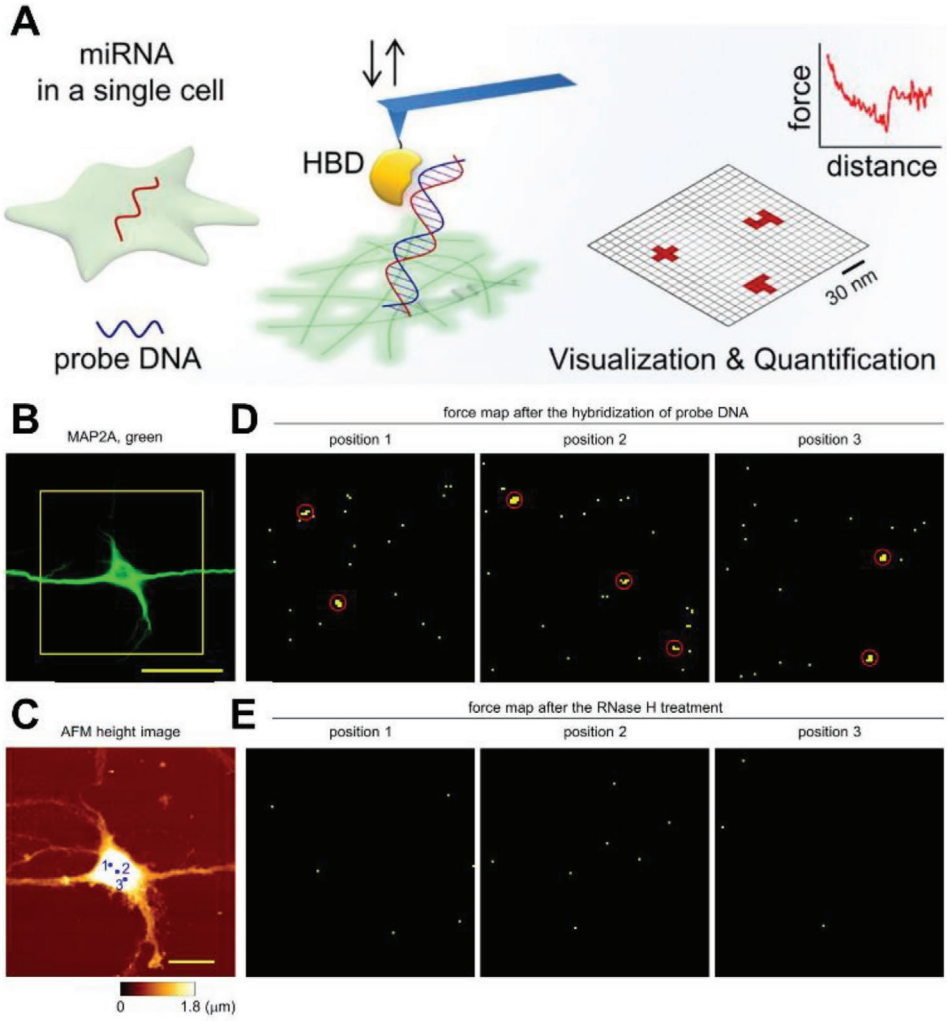


**Figure 9.** Atomic force microscope imaging for intracellular miRNA detection. A) Schematic illustration for miRNA detection in a single cell by tracking the single-molecular adhesion of a HBD. B) Primary hippocampal neurons (DIV7), MAP2; green. C) The boxed area in panel a was imaged with AFM. D) Numbered regions in panel b were examined by adhesion force mapping after the hybridization of miRNA-134 complementary DNA. E) The same regions were re-examined after the RNase H treatment with the same tip, and no cluster was observed. Scale bars: 50 μm in panel B and 20 μm in panel C. Reproduced with permission.[14] Copyright 2016, American Chemical Society.

miRNAs location by the specific curves at a high lateral resolution (Figure 9B–E).

## 5. Conclusion and Challenge

Since the miRNA was discovered in Caenorhabditis elegans in 1993, various miRNAs have been published and recorded in a searchable database and their numbers are still growing. They are relatively new on the scene as critical post-transcriptional regulators of gene expression, and captured the imagination of researchers and stimulated an arouse of activity in design nanoprobes to explore their functions in vivo. Compared to conventional miRNA analysis in vitro, the intracellular miRNA profiling could elucidate spatiotemporal and dynamic physiological and pathological information in intact living cells or tissues. In the review, we introduced various nanoprobes from delivery vehicles, sequence designs, and imaging technologies, aiming to reveal how to design desired nanoprobes for miRNA live-cell analysis. As a proof-of-concept, nanoprobes exhibit the ability to distinguish the different diseased cells and normal cells via single or multiplex intracellular miRNA imagings, even in co-culture dishes. They also could be a non-invasion diagnosis tools to guide the therapy of cancer cell-xenograft-bearing mice.

Despite the advantages and the application potential, there are several issues needed to be addressed for their widespread adoption as clinic diagnosis tools. First and foremost, most of the nanoprobes are absence the clinical verification and evaluation. Although many nanoprobes had been applied in taking cultured tumor cell lines, multicellular tumor spheroids, or cancer cell-xenograft-bearing mice, the simple simulation system in laboratory cannot represent the real clinical samples. Thus, the availability of nanoprobe system need to be further evaluated using clinical samples.

Second, single miRNA analysis cannot provide sufficient evidence for disease diagnosis. For example, it is reported that miRNA-21 exhibited an overexpression in breast cancer, but it cannot identify whether the cancer cells has metastasized.[105] Thus, it is important to ensure the association between various miRNAs and other biomarkers (e.g., telomerase, ATP, and mRNA) for clinical diagnosis. Although there is still a long way to go, we anticipate that miRNA imaging technologies will be widespread applied in clinical diagnosis or developing personalized medicine in the future.

## Acknowledgements

The work was supported by the Excellent Young Scientists Fund (22022407), National Natural Science Foundation of China (21874008, 22004006), the work was also supported by Major Program of National Natural Science Foundation of China (21890740 and 21890742), Special Foundation for State Major Research Program of China (Grant Nos.2019YFC1606603), SZU Top Ranking Project (860000002100165,86000000210), and Beijing Municipal Science and Technology Commission (Grant No. z131102002813058). 2021 Stability support plan of Shenzhen University (8940206/0200). [Correction added on 10 March 2022, after first online publication: Affiliation order changed].

## Conflict of Interest

The authors declare no conflict of interest.

## Keywords

biosensors, delivery vehicles, DNA-based nanoprobes, in situ detection, microRNA imaging

Received: October 15, 2021
Published online: December 2, 2021

[1] T. Jet, G. Gines, Y. Rondelez, V. Taly, *Chem. Soc. Rev.* **2021**, *50*, 4141.
[2] H. Dong, J. Lei, L. Ding, Y. Wen, H. Ju, X. Zhang, *Chem. Rev.* **2013**, *113*, 6207.
[3] A. Kozomara, M. Birgaoanu, S. Griffiths-Jones, *Nucleic Acids Res.* **2019**, *47*, D155.
[4] K. Gumireddy, D. D. Young, X. Xiong, J. B. Hogenesch, Q. Huang, A. Deiters, *Angew. Chem., Int. Ed.* **2008**, *47*, 7482.
[5] a) C. Y. Shi, E. R. Kingston, B. Kleaveland, D. H. Lin, M. W. Stubna, D. P. Bartel, *Science* **2020**, *370*, eabc9359; b) L. Wu, Y. Wang, X. Xu, Y. Liu, B. Lin, M. Zhang, J. Zhang, S. Wan, C. Yang, W. Tan, *Chem. Rev.* **2021**, *121*, 120351.
[6] A. W. Wark, H. J. Lee, R. M. Corn, *Angew. Chem., Int. Ed.* **2008**, *47*, 644.
[7] a) A. Lujambio, S. W. Lowe, *Nature* **2012**, *482*, 347; b) A. L. Kasinski, F. J. Slack, *Nat. Rev. Cancer* **2011**, *11*, 849.
[8] G. Obernosterer, J. Martinez, M. Alenius, *Nat. Protoc.* **2007**, *2*, 1508.
[9] J. Y. Kishi, S. W. Lapan, B. J. Beliveau, E. R. West, A. Zhu, H. M. Sasaki, S. K. Saka, Y. Wang, C. L. Cepko, P. Yin, *Nat. Methods* **2019**, *16*, 533.
[10] a) C. J. Kearney, C. R. Lucas, F. J. O'brien, C. E. Castro, *Adv. Mater.* **2016**, *28*, 5509; b) S. Liu, Q. Jiang, Y. Wang, B. Ding, *Adv. Healthcare Mater.* **2019**, *8*, 1801658; c) Y. Tang, B. Ge, D. Sen, H. Z. Yu, *Chem. Soc. Rev.* **2014**, *43*, 518.
[11] a) H. J. Vaughan, J. J. Green, S. Y. Tzeng, *Adv. Mater.* **2020**, *32*, 1901081; b) D. Samanta, S. B. Ebrahimi, C. A. Mirkin, *Adv. Mater.* **2020**, *32*, 1901743; c) M. Xiao, W. Lai, T. Man, B. Chang, L. Li, A. R. Chandrasekaran, H. Pei, *Chem. Rev.* **2019**, *119*, 11631.
[12] J. J. Xu, W. W. Zhao, S. Song, C. Fan, H. Y. Chen, *Chem. Soc. Rev.* **2014**, *43*, 1601.
[13] W. Ma, P. Fu, M. Sun, L. Xu, H. Kuang, C. Xu, *J. Am. Chem. Soc.* **2017**, *139*, 11752.
[14] H. Koo, I. Park, Y. Lee, H. J. Kim, J. H. Jung, J. H. Lee, Y. Kim, J. H. Kim, J. W. Park, *J. Am. Chem. Soc.* **2016**, *138*, 11664.
[15] K. Zhang, X. Meng, Z. Yang, Y. Cao, Y. Cheng, D. Wang, H. Lu, Z. Shi, H. Dong, X. Zhang, *Adv. Mater.* **2019**, *31*, 1807888.
[16] S. Behzadi, V. Serpooshan, W. Tao, M. A. Hamaly, M. Y. Alkawareek, E. C. Dreaden, D. Brown, A. M. Alkilany, O. C. Farokhzad, M. Mahmoudi, *Chem. Soc. Rev.* **2017**, *46*, 4218.
[17] a) J. Yang, A. Bahreman, G. Daudey, J. Bussmann, R. C. Olsthoorn, A. Kros, *ACS Cent. Sci.* **2016**, *2*, 621; b) H. Pick, A. C. Alves, H. Vogel, *Chem. Rev.* **2018**, *118*, 8598.
[18] C. Xue, S. X. Zhang, C. H. Ouyang, D. Chang, B. J. Salena, Y. Li, Z. S. Wu, *Angew. Chem., Int. Ed.* **2018**, *57*, 9739.
[19] S. Huo, H. Li, A. J. Boersma, A. Herrmann, *Adv. Sci.* **2019**, *6*, 1900043.
[20] a) Z. Ge, H. Gu, Q. Li, C. Fan, *J. Am. Chem. Soc.* **2018**, *140*, 17808; b) F. Yang, Q. Li, L. Wang, G. J. Zhang, C. Fan, *ACS Sens.* **2018**, *3*, 903; c) C. Wiraja, Y. Zhu, D. C. S. Lio, D. C. Yeo, M. Xie, W. Fang, Q. Li, M. Zheng, M. Van Steensel, L. Wang, C. Fan, C. Xu, *Nat. Commun.* **2019**, *10*, 1147; d) N. C. Seeman, H. F. Sleiman, *Nat. Rev. Mater.* **2017**, *3*, 17068.

[21] a) Q. Hu, H. Li, L. Wang, H. Gu, C. Fan, *Chem. Rev.* **2019**, *119*, 6459; b) Y. Wan, N. Zhu, Y. Lu, P. K. Wong, *Anal. Chem.* **2019**, *91*, 2626; c) R. Peng, H. Wang, Y. Lyu, L. Xu, H. Liu, H. Kuai, Q. Liu, W. Tan, *J. Am. Chem. Soc.* **2017**, *139*, 12410; d) J. Huang, W. Ma, H. Sun, H. Wang, X. He, H. Cheng, M. Huang, Y. Lei, K. Wang, *ACS Appl. Bio Mater.* **2020**, *3*, 2779.
[22] a) P. Peng, Y. Du, J. Zheng, H. Wang, T. Li, *Angew. Chem., Int. Ed.* **2019**, *58*, 1648; b) Y. Du, P. Peng, T. Li, *ACS Nano* **2019**, *13*, 5778.
[23] J. Li, H. Pei, B. Zhu, L. Liang, M. Wei, Y. He, N. Chen, D. Li, Q. Huang, C. Fan, *ACS Nano* **2011**, *5*, 8783.
[24] A. S. Walsh, H. Yin, C. M. Erben, M. J. Wood, A. J. Turberfield, *ACS Nano* **2011**, *5*, 5427.
[25] F. Yang, Y. Cheng, Y. Zhang, W. Wei, H. Dong, H. Lu, X. Zhang, *Anal. Chem.* **2020**, *92*, 4411.
[26] X. Fu, G. Ke, F. Peng, X. Hu, J. Li, Y. Shi, G. Kong, X. B. Zhang, W. Tan, *Nat. Commun.* **2020**, *11*, 1518.
[27] a) T. Wu, J. Liu, M. Liu, S. Liu, S. Zhao, R. Tian, D. Wei, Y. Liu, Y. Zhao, H. Xiao, B. Ding, *Angew. Chem., Int. Ed.* **2019**, *58*, 14224; b) Y. Zhang, W. Ma, Y. Zhu, S. Shi, Q. Li, C. Mao, D. Zhao, Y. Zhan, J. Shi, W. Li, L. Wang, C. Fan, Y. Lin, *Nano Lett.* **2018**, *18*, 5652.
[28] Q. Jiang, S. Liu, J. Liu, Z. G. Wang, B. Ding, *Adv. Mater.* **2019**, *31*, 1804785.
[29] a) H. M. Meng, X. Zhang, Y. Lv, Z. Zhao, N. N. Wang, T. Fu, H. Fan, H. Liang, L. Qiu, G. Zhu, W. Tan, *ACS Nano* **2014**, *8*, 6171; b) C. Wu, D. Han, T. Chen, L. Peng, G. Zhu, M. You, L. Qiu, K. Sefah, X. Zhang, W. Tan, *J. Am. Chem. Soc.* **2013**, *135*, 18644.
[30] a) H. Yang, H. A. Clark, *Chem* **2019**, *5*, 1687; b) Y. Lyu, Y. Guo, R. Cai, R. Peng, C. Hong, X. Chen, W. Hou, X. Li, J. Tan, Y. Zou, X. Zhang, Q. Liu, W. Tan, *Chem* **2019**, *5*, 913.
[31] R. P. Chen, D. Blackstock, Q. Sun, W. Chen, *Nat. Chem.* **2018**, *10*, 474.
[32] a) C. Hartl, K. Frank, H. Amenitsch, S. Fischer, T. Liedl, B. Nickel, *Nano Lett.* **2018**, *18*, 2609; b) Y. Li, Z. Liu, G. Yu, W. Jiang, C. Mao, *J. Am. Chem. Soc.* **2015**, *137*, 4320; c) T. Trinh, C. Liao, V. Toader, M. Barlog, H. S. Bazzi, J. Li, H. F. Sleiman, *Nat. Chem.* **2018**, *10*, 184.
[33] K. Ren, Y. Zhang, X. Zhang, Y. Liu, M. Yang, H. Ju, *ACS Nano* **2018**, *12*, 10797.
[34] S. Li, L. Xu, M. Sun, X. Wu, L. Liu, H. Kuang, C. Xu, *Adv. Mater.* **2017**, *29*, 1606086.
[35] H. Dong, J. Lei, H. Ju, F. Zhi, H. Wang, W. Guo, Z. Zhu, F. Yan, *Angew. Chem., Int. Ed.* **2012**, *51*, 4607.
[36] W. Dai, H. Dong, K. Guo, X. Zhang, *Chem. Sci.* **2018**, *9*, 1753.
[37] E. Kim, J. Yang, J. Park, S. Kim, N. H. Kim, J. I. Yook, J. S. Suh, S. Haam, Y. M. Huh, *ACS Nano* **2012**, *6*, 8525.
[38] Z. Fan, K. Xiao, J. Lin, Y. Liao, X. Huang, *Small* **2019**, *15*, 1903761.
[39] N. Panwar, A. M. Soehartono, K. K. Chan, S. Zeng, G. Xu, J. Qu, P. Coquet, K. T. Yong, X. Chen, *Chem. Rev.* **2019**, *119*, 9559.
[40] a) F. Yang, P. Liu, X. Meng, H. Lu, Y. Cao, W. Dai, C. Wang, H. Dong, *Anal. Bioanal. Chem.* **2019**, *411*, 4559; b) Y. Cao, H. Dong, Z. Yang, X. Zhong, Y. Chen, W. Dai, X. Zhang, *ACS Appl. Mater. Interfaces* **2017**, *9*, 159.
[41] E. K. Lim, T. Kim, S. Paik, S. Haam, Y. M. Huh, K. Lee, *Chem. Rev.* **2015**, *115*, 327.
[42] Y. Wu, J. Huang, X. Yang, Y. Yang, K. Quan, N. Xie, J. Li, C. Ma, K. Wang, *Anal. Chem.* **2017**, *89*, 8377.
[43] J. T. Yi, T. T. Chen, J. Huo, X. Chu, *Anal. Chem.* **2017**, *89*, 12351.
[44] Q. Lu, D. Ericson, Y. Song, C. Zhu, R. Ye, S. Liu, J. A. Spernyak, D. Du, H. Li, Y. Wu, Y. Lin, *ACS Appl. Mater. Interfaces* **2017**, *9*, 23325.
[45] X. Wang, Y. Yuan, Z. Wu, J.-H. Jiang, *ACS Appl. Bio Mater.* **2020**, *3*, 2597.
[46] D. Zhu, J. Huang, B. Lu, Y. Zhu, Y. Wei, Q. Zhang, X. Guo, L. Yuwen, S. Su, J. Chao, L. Wang, *ACS Appl. Mater. Interfaces* **2019**, *11*, 20725.
[47] M. R. Cui, X. L. Li, J. J. Xu, H. Y. Chen, *Chem. Commun.* **2019**, *55*, 13366.
[48] Y. Song, X. Yan, G. Ostermeyer, S. Li, L. Qu, D. Du, Z. Li, Y. Lin, *Anal. Chem.* **2018**, *90*, 10369.
[49] X. Liao, Q. Wang, H. Ju, *Chem. Commun.* **2014**, *50*, 13604.
[50] J. Liu, T. Zheng, Y. Tian, *Angew. Chem., Int. Ed.* **2019**, *58*, 7757.
[51] G. Liu, H. Chai, Y. Tang, P. Miao, *Chem. Commun.* **2020**, *56*, 1175.
[52] W. Dai, H. Dong, B. Fugetsu, Y. Cao, H. Lu, X. Ma, X. Zhang, *Small* **2015**, *11*, 4158.
[53] Y. Cao, H. Dong, S. Pu, X. Zhang, *Nano Res.* **2018**, *11*, 4074.
[54] H. Dong, W. Dai, H. Ju, H. Lu, S. Wang, L. Xu, S. F. Zhou, Y. Zhang, X. Zhang, *ACS Appl. Mater. Interfaces* **2015**, *7*, 11015.
[55] C. K. Choi, J. Li, K. Wei, Y. J. Xu, L. W. Ho, M. Zhu, K. K. To, C. H. Choi, L. Bian, *J. Am. Chem. Soc.* **2015**, *137*, 7337.
[56] J. Zhao, H. Chu, Y. Zhao, Y. Lu, L. Li, *J. Am. Chem. Soc.* **2019**, *141*, 7056.
[57] J. Zhang, M. He, C. Nie, M. He, Q. Pan, C. Liu, Y. Hu, J. Yi, T. Chen, X. Chu, *Anal. Chem.* **2019**, *91*, 9049.
[58] H. Xiao, H. Fan, L. Xu, Z. Pei, S. Lei, J. Xu, J. Xi, G. Wang, L. Wang, Z. Wang, *Chem. Commun.* **2019**, *55*, 12352.
[59] C. Liu, C. Chen, S. Li, H. Dong, W. Dai, T. Xu, Y. Liu, F. Yang, X. Zhang, *Anal. Chem.* **2018**, *90*, 10591.
[60] N. Yan, X. Wang, L. Lin, T. Song, P. Sun, H. Tian, H. Liang, X. Chen, *Adv. Funct. Mater.* **2018**, *28*, 1800490.
[61] X. Cao, Z. Wang, L. Bi, C. Bi, Q. Du, *Nanoscale* **2020**, *12*, 1513.
[62] H. Lu, F. Yang, B. Liu, K. Zhang, Y. Cao, W. Dai, W. Li, H. Dong, *Nanoscale Horiz.* **2019**, *4*, 472.
[63] a) P. L. Felgner, G. M. Ringold, *Nature* **1989**, *337*, 387; b) W. T. Al-Jamal, K. Kostarelos, *Acc. Chem. Res.* **2011**, *44*, 1094; c) S. Han, B. Kang, E. Jang, J. Ki, E. Kim, M.-Y. Jeong, Y.-M. Huh, H.-Y. Son, S. Haam, *Adv. Healthcare Mater.* **2018**, *7*, 1701019.
[64] H. Peng, A. M. Newbigging, M. S. Reid, J. S. Uppal, J. Xu, H. Zhang, X. C. Le, *Anal. Chem.* **2020**, *92*, 292.
[65] J. Wei, H. Wang, X. Gong, Q. Wang, H. Wang, Y. Zhou, F. Wang, *Nucleic Acids Res.* **2020**, *48*, e60.
[66] Z. Yang, S. Zhang, H. Zhao, H. Niu, Z. S. Wu, H. T. Chang, *Anal. Chem.* **2018**, *90*, 13891.
[67] a) Z. Wang, Y. Yang, Z. Xu, Y. Wang, W. Zhang, P. Shi, *Nano Lett.* **2015**, *15*, 7058; b) Z. Wang, L. Qi, Y. Yang, M. Lu, K. Xie, X. Zhao, E. H. C. Cheung, Y. Wang, X. Jiang, W. Zhang, L. Huang, X. Wang, P. Shi, *Sci. Adv.* **2020**, *6*, eaba4971.
[68] Y. Wang, Y. Yang, L. Yan, S. Y. Kwok, W. Li, Z. Wang, X. Zhu, G. Zhu, W. Zhang, X. Chen, P. Shi, *Nat. Commun.* **2014**, *5*, 4466.
[69] K. Xie, Z. Wang, L. Qi, X. Zhao, Y. Wang, J. Qu, P. Xu, L. Huang, W. Zhang, Y. Yang, X. Wang, P. Shi, *ACS Nano* **2021**, *15*, 4881.
[70] J. Zhao, Z. Li, Y. Shao, W. Hu, L. Li, *Angew. Chem., Int. Ed.* **2021**, *60*, 17937.
[71] C. P. Liang, P. Q. Ma, H. Liu, X. Guo, B. C. Yin, B. C. Ye, *Angew. Chem., Int. Ed.* **2017**, *56*, 9077.
[72] F. Yang, Y. Cheng, Y. Cao, Y. Zhang, H. Dong, H. Lu, X. Zhang, *Anal. Chem.* **2019**, *91*, 9828.
[73] L. Xian, F. Xu, J. Liu, N. Xu, H. Li, H. Ge, K. Shao, J. Fan, G. Xiao, X. Peng, *J. Am. Chem. Soc.* **2019**, *141*, 20490.
[74] a) W. Wang, *Chem. Soc. Rev.* **2018**, *47*, 2485; b) X. Huang, J. Song, B. C. Yung, X. Huang, Y. Xiong, X. Chen, *Chem. Soc. Rev.* **2018**, *47*, 2873; c) J. Li, F. Cheng, H. Huang, L. Li, J. J. Zhu, *Chem. Soc. Rev.* **2015**, *44*, 7855.
[75] S. L. Liu, Z. G. Wang, H. Y. Xie, A. A. Liu, D. C. Lamb, D. W. Pang, *Chem. Rev.* **2020**, *120*, 1936.
[76] X. Meng, K. Zhang, W. Dai, Y. Cao, F. Yang, H. Dong, X. Zhang, *Chem. Sci.* **2018**, *9*, 7419.
[77] H. Wang, C. Li, X. Liu, X. Zhou, F. Wang, *Chem. Sci.* **2018**, *9*, 5842.
[78] Z. M. Ying, Z. Wu, B. Tu, W. Tan, J. H. Jiang, *J. Am. Chem. Soc.* **2017**, *139*, 9779.
[79] A. Qu, L. Xu, M. Sun, L. Liu, H. Kuang, C. Xu, *Adv. Funct. Mater.* **2017**, *27*, 1703408.

[80] a) X. Zhao, L. Xu, M. Sun, W. Ma, X. Wu, H. Kuang, L. Wang, C. Xu, *Small* **2016**, *12*, 4662; b) K. D. Wegner, N. Hildebrandt, *Chem. Soc. Rev.* **2015**, *44*, 4792; c) G. Yang, S. Z. F. Phua, A. K. Bindra, Y. Zhao, *Adv. Mater.* **2019**, *31*, 1805730.
[81] a) P. Zrazhevskiy, M. Sena, X. Gao, *Chem. Soc. Rev.* **2010**, *39*, 4326; b) G. Wang, Z. Li, N. Ma, *ACS Chem. Biol.* **2018**, *13*, 1705.
[82] X. He, T. Zeng, Z. Li, G. Wang, N. Ma, *Angew. Chem., Int. Ed.* **2016**, *128*, 3125.
[83] A. Qu, M. Sun, L. Xu, C. Hao, X. Wu, C. Xu, N. A. Kotov, H. Kuang, *Proc. Natl. Acad. Sci. U. S. A.* **2019**, *116*, 3391.
[84] L. Yang, K. Zhang, S. Bi, J. J. Zhu, *ACS Appl. Mater. Interfaces* **2019**, *11*, 38459.
[85] B. R. Smith, S. S. Gambhir, *Chem. Rev.* **2017**, *117*, 901.
[86] L. Xu, S. Zhao, W. Ma, X. Wu, S. Li, H. Kuang, L. Wang, C. Xu, *Adv. Funct. Mater.* **2016**, *26*, 1602.
[87] X. Guo, J. Li, M. Arabi, X. Wang, Y. Wang, L. Chen, *ACS Sens.* **2020**, *5*, 601.
[88] C. Li, S. Li, A. Qu, H. Kuang, L. Xu, C. Xu, *Adv. Funct. Mater.* **2020**, *30*, 2001451.
[89] a) X. Song, Y. Wang, F. Zhao, Q. Li, H. Q. Ta, M. H. Rummeli, C. G. Tully, Z. Li, W. J. Yin, L. Yang, K. B. Lee, J. Yang, I. Bozkurt, S. Liu, W. Zhang, M. Chhowalla, *ACS Nano* **2019**, *13*, 8312; b) C. Zhang, P. Miao, M. Sun, M. Yan, H. Liu, *Small* **2019**, *15*, 1901867.
[90] W. Ma, M. Sun, P. Fu, S. Li, L. Xu, H. Kuang, C. Xu, *Adv. Mater.* **2017**, *29*, 1703410.
[91] Y. Liu, P. Bhattarai, Z. Dai, X. Chen, *Chem. Soc. Rev.* **2018**, *48*, 2053.
[92] X. L. Dean-Ben, S. Gottschalk, B. Mc Larney, S. Shoham, D. Razansky, *Chem. Soc. Rev.* **2017**, *46*, 2158.
[93] T. Kim, Q. Zhang, J. Li, L. Zhang, J. V. Jokerst, *ACS Nano* **2018**, *12*, 5615.
[94] W. Cao, W. Gao, Z. Liu, W. Hao, X. Li, Y. Sun, L. Tong, B. Tang, *Anal. Chem.* **2018**, *90*, 9125.
[95] a) L. Zhang, J. Wang, J. Zhang, Y. Liu, L. Wu, J. Shen, Y. Zhang, Y. Hu, Q. Fan, W. Huang, L. Wang, *ACS Sens.* **2017**, *2*, 1435; b) Y. Gu, J. Song, M. X. Li, T. T. Zhang, W. Zhao, J. J. Xu, M. Liu, H. Y. Chen, *Anal. Chem.* **2017**, *89*, 10585; c) S. Kim, J. E. Park, W. Hwang, J. Seo, Y. K. Lee, J. H. Hwang, J. M. Nam, *J. Am. Chem. Soc.* **2017**, *139*, 3558.
[96] a) Y. Ling, D. Zhang, X. Cui, M. Wei, T. Zhang, J. Wang, L. Xiao, Y. Xia, *Angew. Chem., Int. Ed.* **2019**, *58*, 10542; b) Z. Chen, J. Li, X. Chen, J. Cao, J. Zhang, Q. Min, J. J. Zhu, *J. Am. Chem. Soc.* **2015**, *137*, 1903.
[97] J. Shen, L. Liang, M. Xiao, X. Xie, F. Wang, Q. Li, Z. Ge, J. Li, J. Shi, L. Wang, L. Li, H. Pei, C. Fan, *J. Am. Chem. Soc.* **2019**, *141*, 11938.
[98] a) Y. Li, C. Jing, L. Zhang, Y. T. Long, *Chem. Soc. Rev.* **2012**, *41*, 632; b) A. Kumar, S. Kim, J. M. Nam, *J. Am. Chem. Soc.* **2016**, *138*, 14509.
[99] Y. K. Lee, S. Kim, J. W. Oh, J. M. Nam, *J. Am. Chem. Soc.* **2014**, *136*, 4081.
[100] a) M. X. Li, C. H. Xu, N. Zhang, G. S. Qian, W. Zhao, J. J. Xu, H. Y. Chen, *ACS Nano* **2018**, *12*, 3341; b) T. Chen, Y. Hong, B. M. Reinhard, *Nano Lett.* **2015**, *15*, 5349.
[101] Y. W. Jun, S. Sheikholeslami, D. R. Hostetter, C. Tajon, C. S. Craik, A. P. Alivisatos, *Proc. Natl. Acad. Sci. U. S. A.* **2009**, *106*, 17735.
[102] M. X. Li, W. Zhao, H. Wang, X. L. Li, C. H. Xu, H. Y. Chen, J. J. Xu, *Anal. Chem.* **2018**, *90*, 14255.
[103] C. M. Platnich, F. J. Rizzuto, G. Cosa, H. F. Sleiman, *Chem. Soc. Rev.* **2020**, *49*, 4220.
[104] S. Husale, H. H. Persson, O. Sahin, *Nature* **2009**, *462*, 1075.
[105] M. Bai, F. Chen, X. Cao, Y. Zhao, J. Xue, X. Yu, C. Fan, Y. Zhao, *Angew. Chem., Int. Ed.* **2020**, *59*, 13267.

**Fan Yang** received her Ph.D. degree in chemistry from University of Science and Technology Beijing in 2021. She then joined college of basic medical sciences at Shanxi Medical University as a Lecturer in 2021. Her current research is focused on developing novel nucleic acid probes for intracellular microRNA imaging.

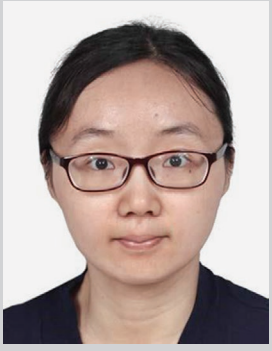

**Huiting Lu** received her Ph.D. from Beihang University in Materials Physics and Chemistry in 2017. She is currently a Postdoctoral Researcher at University of Science and Technology Beijing. Her research interests include synthesizing nanoparticles and their behavior and toxicity in environment.

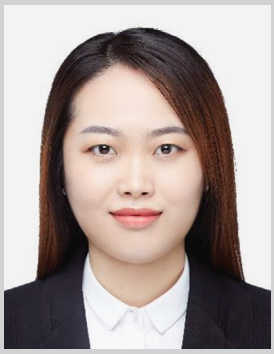

**Xiangdan Meng** received her Ph.D. degree in chemistry in 2019 from University of Science and Technology Beijing. Then she joined the Research Center for Bioengineering and Sensing Technology research group at University of Science and Technology Beijing as a postdoctoral researcher. Her current research interests include the design of functional nanoprobes, biosensors, and nanomedicine.

**Haifeng Dong** received his Ph.D. degree from Nanjing University in 2011. He then joined the USTB in the same year. He pursued his research as a postdoctoral researcher at the University of Pittsburgh from 2012. to 2013. Afterward, he joined University of Science and Technology Beijing as a Professor. He works as a Visiting Professor of Kyoto University during 2015. to 2015. He moved to Shenzhen University as a Professor on 2020. His research interests include the application of functional nanoprobes in DNA biosensors and imaging analysis of intracellular microRNA, as well as, nanomedicine.

**Xueji Zhang** is the Vice President of Shenzhen University. He received his Ph.D. degree from Wuhan University in 1994, and was a postdoctoral scholar at the National Institute of Chemistry Slovenia from 1995 to 1997, Swiss Federal Institute of Technology from 1997 to 1998, and New Mexico State University from 1998 to 1999. He joined the World Precision Instruments Inc. as a Sr. Scientist, Head of the Chemistry Department in 1999, and then became the Senior Vice President in 2004. His current research focuses on bioanalysis, electrochemical sensors, micro/nanosensors, and biomedical instrumentation.